Raman effects under pressure in chloroadamantane plastic crystal

2002 J. Phys.: Condens. Matter 14 8725

(http://iopscience.iop.org/0953-8984/14/37/309)

INSTITUTE OF PHYSICS PUBLISHING JOURNAL OF PHYSICS: CONDENSED MATTER

J. Phys.: Condens. Matter **14** (2002) 8725–8741 PII: S0953-8984(02)37387-9

Raman effects under pressure in chloroadamantane plastic crystal

A Hédoux, Y Guinet, F Capet, F Affouard and M Descamps

Laboratoire de Dynamique et Structure des Matériaux Moléculaires, ESA CNRS 8024, Université des Sciences et Technologies de Lille, 59655 Villeneuve d'Ascq Cédex, France

E-mail: alain.hedoux@univ-lille1.fr

Received 23 May 2002, in final form 2 July 2002
Published 5 September 2002
Online at stacks.iop.org/JPhysCM/14/8725

Abstract

Raman scattering experiments have been performed on orientationally disordered crystal chloroadamantane under pressure. Investigations carried out in both the lattice-mode and the internal-mode regions have shown that this plastic crystal exhibits spectroscopic features common to most molecular solids. The pressure-induced disorder–order phase transition around 0.5 GPa has been analysed using crystallographic and Raman data in the low-temperature phase. Additional features were observed with further compression above 8 GPa. Two different hypotheses are proposed to explain these features.

1. Introduction

Orientationally disordered molecular solids have been widely investigated during the last few decades because some of them, such as cyanoadamantane (CNa) [1], ethanol [2, 3], cyclooctanol [4], and difluorotetrachloroethane [5], can be supercooled into a metastable state and then vitrified. The lengthening timescale for diffusional or reorientational motions, at the origin of the glass transition, was analysed within the framework of the 'strong' and 'fragile' classification of both liquids and plastic crystals [6, 7]. Glassy crystals have numerous similarities with the conventional glassy state, and plastic crystals give an additional opportunity to obtain a fundamental understanding of glass formation. More recent investigations on the substituted adamantane family have revealed, from molecular dynamics simulations, that the dynamics of chloroadamantane $C_{10}H_{15}Cl$ (Cla) was relatively well described by mode-coupling theory [8]. In Cla, several experimental features [9, 10] converge to suggest a crossover temperature, near 330 K, indicative of a dynamical transition between quasi-free diffusion and an activated regime as predicted for glass-forming liquids [11]. Local orientational ordering can be detected in the plastic phase below 330 K, from the analysis of the temperature dependence of the so-called bending mode of Cla [10], by means of Raman scattering investigations.

It is also well known that some non-thermal constraints can induce polymorphic and polyamorphic transitions. In several disordered molecular solids, an disorder–order (plastic–brittle) transition is induced at high pressure. Indeed, adamantane $C_{10}H_{16}$ (adm) is known to exhibit a transition to an orientationally ordered state at low temperature [12] as well as at high pressure [13]. From FT-IR investigations a phase transition was detected in Cla near 5 kbar [14], and assigned to the disorder–order transition observed at ambient pressure by lowering the temperature below 260 K. Both in adamantane [13] and in chloroadamantane [14] additional transitions are observed on increasing pressure. On the other hand, pressure-induced amorphization is observed in plastic crystals such as C_{60} [15] and C_{70} [16], and liquid–liquid transition can also be induced at high pressure [17, 18]. Consequently, investigations in the high-pressure range of plastic crystals can provide information about the ordering process, glass formation, and the polyamorphism phenomenon.

The aim of the present work is to investigate the high-pressure polymorphism of Cla, on the basis of low-frequency Raman scattering experiments performed in the ambient pressure to 12 GPa range, since only the spectral region above 600 cm^{-1} has been investigated by infrared spectroscopy within a narrow pressure range ($P < 4$ GPa) [14]. The high-pressure phase can be rigorously compared to the low-temperature one using symmetry considerations, and its stability under pressurizing as well as its ability to show pressure-induced amorphization are further investigated.

2. Experimental details

Experiments were performed at room temperature on a single crystal of Cla grown by the sublimation method. Pressure was generated in a gasketed membrane diamond-anvil cell (MDAC). Measurements were carried out without any pressure-transmitting medium. The sample size was typically 200 μm diameter and 120 μm thickness. Three ruby crystals (size: $\sim$10 μm) were included for *in situ* pressure measurements by the standard fluorescence technique [18] with an accuracy of $\pm$0.1 GPa. Three pressure runs were carried out, reaching a maximum pressure of 12.5 GPa with a homogeneous distribution of measurements in the 0–12.5 GPa pressure range. Pressure measurements on the three ruby crystals indicate that pressure gradients in the sample were insignificant over the range 0–12.5 GPa. The 514.5 nm line of a mixed argon–krypton laser was used for Raman excitation. The laser beam was focused using a long-working-distance objective ($\times$50) of an Olympus microscope. The back-scattering spectra were recorded using a DILOR-XY spectrometer equipped with a liquid-nitrogen-cooled charge-coupled-device detector. The spectrometer slits were kept at 150 μm which gives a resolution-limited width of 1.3 cm^{-1}. The 5–500 cm^{-1} frequency range was investigated over the 0–12.5 GPa pressure range.

3. Results

The high-pressure dependence of the Raman spectrum over the 5–500 cm^{-1} range (figure 1) was investigated. In this spectral window, two distinct spectral regions are distinguishable. These are the lattice-mode and the internal-mode regions.

(i) In Cla the lattice-mode region lies in the low-frequency range below 150 cm^{-1} at ambient pressure (figure 1(a)). The low-frequency Raman susceptibility in the plastic phase was observed to be dominated by a broad feature—i.e. a phonon density of states, as expected for a highly disordered system.

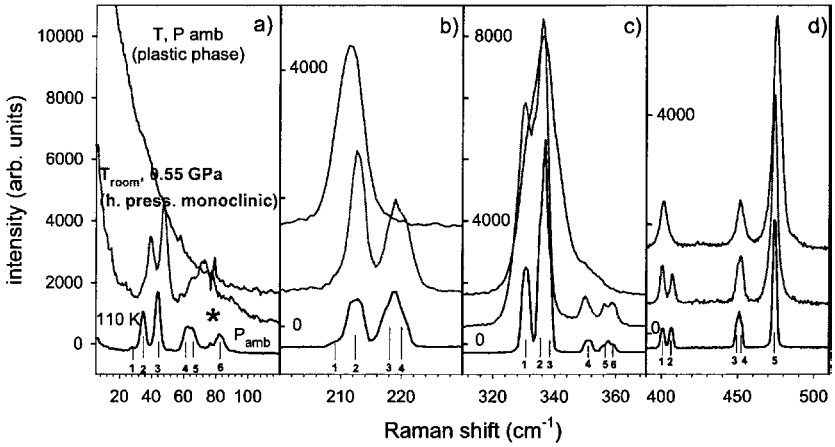

Figure 1. Raman spectra of the lattice modes (a) and internal modes (b)–(d) in the plastic phase at room temperature and atmospheric pressure, and in the ordered phase obtained either at room temperature by pressurization ($P = 0.55$ GPa), or at atmospheric pressure by lowering the temperature (110 K). The asterisk indicates the laser line. The Raman-mode count is marked in each spectral region.

(ii) The isolated 1-chloroadamantane molecule ($C_{10}H_{15}Cl$) has C_{3v} symmetry and possesses 72 internal modes in the plastic phase ($Fm3m$, $Z = 4$) as for the free molecule:

$$\Gamma_{int} = 16A_1 + 8A_2 + 24E.$$

The internal-mode region can be divided into three spectral windows in the range investigated, extending over 500 cm^{-1}:

- In the 200–250 cm^{-1} region (figure 1(b)) the internal E mode, corresponding to the C–Cl distortion with respect to the molecular axis (the so-called bending mode), is observed near 210 cm^{-1} at ambient pressure. This mode appears very interesting because it is Raman active in an isolated spectral window, and it is a very sensitive probe of the local ordering [10, 21].
- The most intense internal vibrational band of the Raman spectrum around 335 cm^{-1} (figure 1(c)). In the 300–370 cm^{-1} range, four Raman peaks overlap in the plastic phase.
- In contrast to the situation in figure 1(c), in the (400, 500 cm^{-1}) spectral range (figure 1(d)), three well-separated modes are observed.

3.1. Disorder–order phase transition

Cla undergoes the disorder–order phase transition on lowering the temperature to 246 K at atmospheric pressure. The unit cell of the ordered low-temperature phase of Cla is monoclinic ($P2_1/c$, $Z = 2$) [20]. The Raman spectra of the disordered, the low-temperature, and the high-pressure ordered phases are displayed for the whole spectral range investigated in figure 1.

(i) The relationship between the lineshape of the low-frequency spectrum of the plastic phase and the lattice modes of the ordered phase was recently discussed [10]. It was determined that the broad low-frequency band was composed of two components. The lowest-frequency component was assigned to reorientational molecular motions characteristic of the rotator phase, whereas the high-frequency component was observed to correspond to the envelope of the lattice modes of the ordered phase. In figure 2(a) we report the pressure

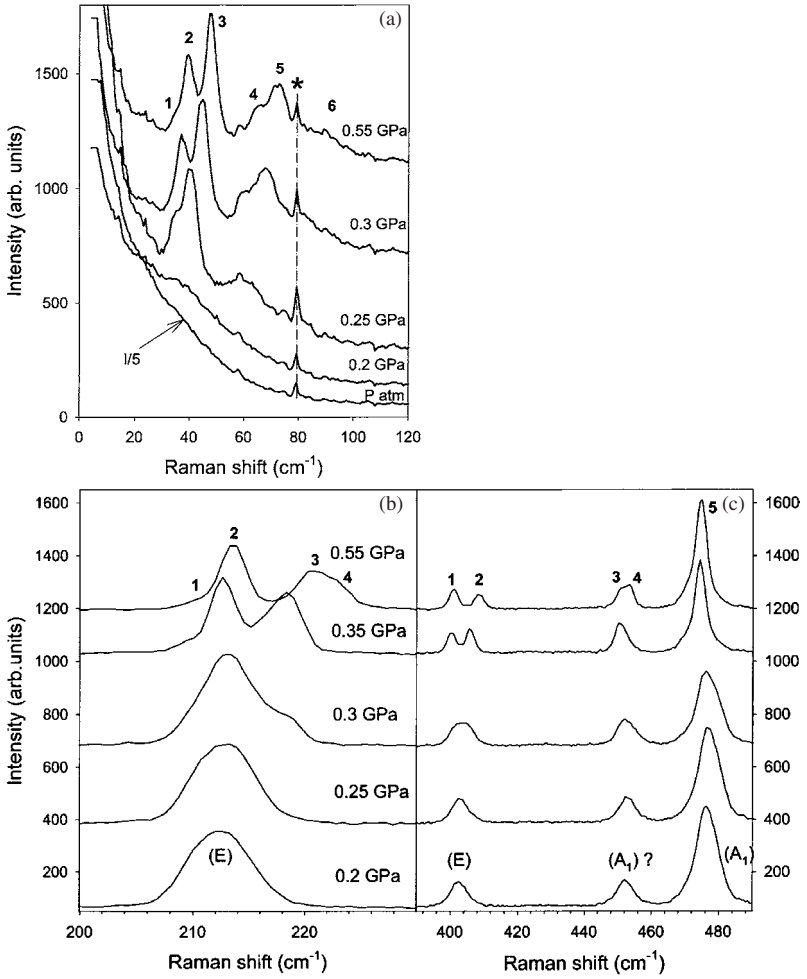

Figure 2. Raman spectra at various pressures in the vicinity of the disorder–order phase transition of chloroadamantane (a) in the lattice-mode region (the asterisk indicates the laser line); (b) in the bending-mode region; (c) in the 390–500 cm^{-1} range where three well-defined modes are observed. The symmetry assignment reported in this figure for internal modes was based on a Raman investigation on cyanoadamantane [20] for the bending-mode region and on the present analysis for both internal-mode regions.

dependence of the Raman intensity when the sample is pressurized. It is clearly observed that the Rayleigh wing sharpens with increasing pressure and a tail can be distinguished around 40 cm^{-1}, nearly corresponding to the high-frequency component in the plastic phase at atmospheric pressure. With further pressure increase, six lattice modes emerge from this tail. This observation is consistent with predictions of group theory analysis made using crystallographic data [20]:

$$\Gamma_{ext}^{opt} = \begin{cases} 3A_g + 3B_g & \text{Raman active} \\ + 2A_u + B_u & \text{IR active.} \end{cases}$$

Six well-resolved lattice modes are also observed in the low-temperature spectrum of the ordered phase (figure 1(a)). From the analysis of figures 1(a) and 2(a), it can be assumed that the disordered phase was completely transformed into the ordered phase at 0.55 GPa

where the six Raman-active modes are observed. Consequently it appears from figure 2(a) that compression leads to slow ordering over the (0, 0.55 GPa) pressure range.

(ii) On lowering the crystalline symmetry at the phase transition, the internal modes of the molecule transform as

$$\Gamma_{int} = 72A_g + 72B_g + 72A_u + 72B_u.$$

with the g mode being Raman active and the u modes IR active (table 1). From table 1, each E mode is expected to split into two non-degenerate A modes (under C_1 site symmetry) and each A mode should split into a zone-centre quartet $A_g + B_g + A_u + B_u$ (under C_{2h} crystalline symmetry) in which only g modes are Raman active. To summarize, each E mode of the free molecule can give rise to four Raman-active components ($2(1A_g + 1B_g)$), and each A_1 mode to a doublet ($1A_g + 1B_g$) in the ordered phase. However, it is worth pointing out that the C_3 molecular axes are merely slightly tilted out the crystal planes ($x = 1/4$ and $x = 3/4$), and the site symmetry can be roughly considered as C_{1h}. In this context, E modes can be expected to split into a doublet ($1A_g + 1B_g$) and A_1 modes can undergo no splitting in the ordered phase. Only some internal modes sensitive to the orientation of the C_3 molecular axis can split, as predicted by table 1(a), and the others behave as expected by table 1(b). A significant broadening of the molecular E (C–C=Cl) internal bending mode is observed as the sample is pressurized at 0.2 GPa (figure 2(b)). This broadening appears as a precursor of the splitting of the bending mode into three distinctive bands. This observation confirms that the ordering process appears as a slow transformation with pressurization. It is worth pointing out that four bands can be detected in the ordered phase at 0.55 GPa (counting the broadening tail on the low-frequency side of the most intense bending mode), as observed in the ordered low-temperature phase (figure 1(b)), as could be expected from the symmetry considerations mentioned above (table 1(a)). The low-frequency bending mode will not be analysed because of its very weak intensity and its localization in the wing of the most intense band.

- The broad band observed in the 330–400 cm^{-1} spectral range, is only satisfactorily fitted with four internal modes under ambient conditions (T, P). Six Raman peaks are detected in the high-pressure ordered phase from the fitting procedure. From the relationship between Raman bands in the plastic phase and those observed both in the low-temperature and in the high-pressure ordered phases, the intramolecular modes of the free molecule of Cla were tentatively identified (table 2). The extreme difficulty of assigning a molecular symmetry to these internal modes (because six Raman peaks overlap in a narrow range) demonstrates that no clear information can be obtained with further compression, and no detailed investigation will be reported at higher pressure in this frequency range.
- In the 400–500 cm^{-1} region, three well-separated modes (around 400, 450, and 475 cm^{-1}) are Raman active in the plastic phase (figure 1(d)). In contrast to the pressure behaviour of the bending mode, the 400 cm^{-1} mode is clearly observed to split into two components through a pressure-induced phase transition (figure 2(c)). The 450 cm^{-1} peak seems also to split into a non-resolved doublet, whereas the 475 cm^{-1} peak does not split. One can note in figure 2(c) the frequency discontinuity and the sharpening of this mode through the phase transition. The 475 cm^{-1} can be reasonably assigned to A_1 symmetry because no splitting is predicted for the A_1 mode from table 1(b). The 400 cm^{-1} mode which exhibits a well-resolved doublet can be assigned as an E mode whereas the 450 cm^{-1} mode can be tentatively assigned as an A_1 mode because the split modes are not well separated. It is clear that the number of internal modes is smaller than that expected from table 1(a). This feature confirms that the site symmetry is roughly C_{1h}. All observations and assignments

Table 1. The correlation table for internal modes of the ordered phase of chloroadamantane; (a) from rigorous C_1 site symmetry; (b) from the rough C_{1h} site symmetry.

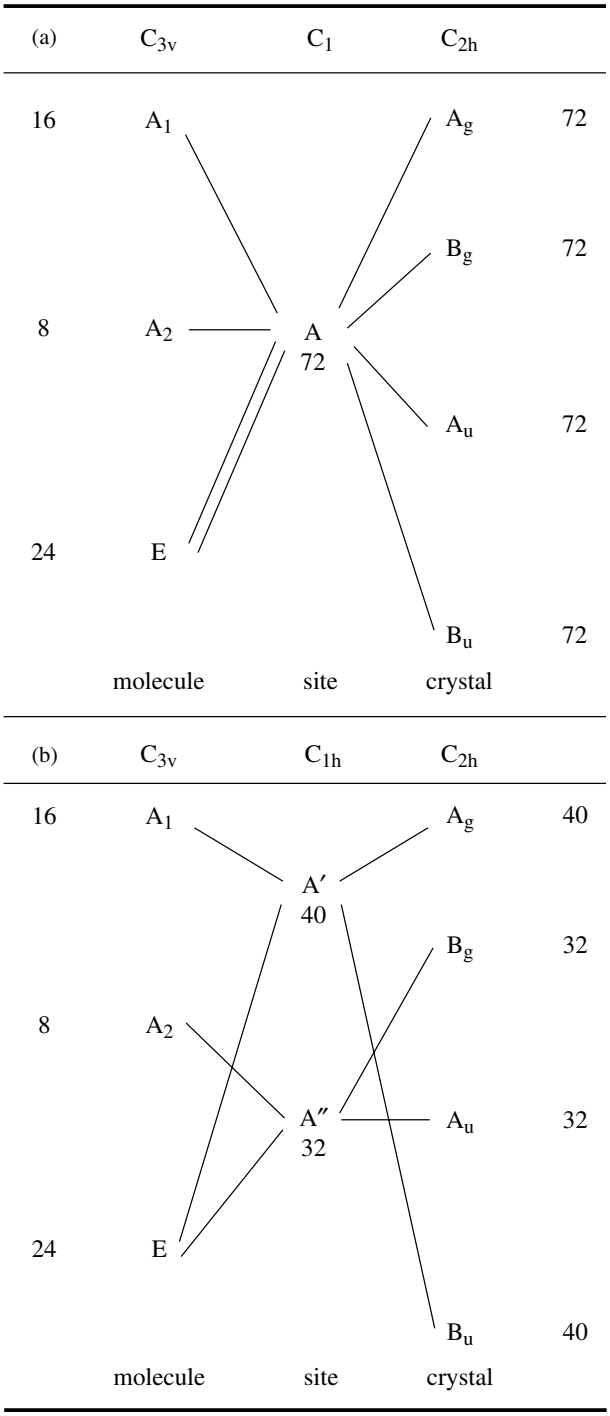

Table 2. The pressure dependence of the lattice modes and some internal modes (below 500 cm^{-1}) in the ordered phase of Cla.

P ambient		$P < 3$ GPa			$P > 3$ GPa
ω (cm^{-1})	(symmetry)	ω (cm^{-1})	(symmetry)	$d\omega/dP$ (cm^{-1} GPa^{-1})	$d\omega/dP$ (cm^{-1} GPa^{-1})
35		29.7	—	7.0(4)	—
		37.1	—	8.4(4)	3.5(2)
		44.8	—	11.5(6)	5.0(3)
		59.4	—	13.7(7)	4.6(2)
		68.1	—	15.8(8)	7.3(4)
		77.1	—	18.7(9)	8.9(4)
212.0	(E)	211.6	(B_g)	1.8(1)	—
		215.6	(A_g)	5.3(3)	—
		217.1	(A_g)	5.8(3)	—
332.0	(A_1)	330	(A_g)	1.0(1)	—
335.5	(E)	334.5	—	0.9(1)	—
		336.5	—	0.9(1)	—
344.2	(A_1)	349.5	(A_g)	1.3(1)	—
353.2	(E)	355.6	—	1.6(1)	—
		357.9	—	2.7(1)	—
401.0	(E)	400.0	—	0.9(1)	—
		405.1	—	3.9(2)	—
450.5	(A_1)	449.9	—	0.8(1)	—
		452.1	—	1.4(1)	—
478.2	(A_1)	473.6	(A_g)	1.1(1)	—

for the high-pressure ordered phase appear consistent with the low-temperature spectrum in this spectral region (figure 1(d)).

3.2. High-pressure behaviour

In ordered phases, the frequencies of all the Raman modes increase monotonically with increasing pressure.

(i) In figure 3(a) we report the pressure dependence of the low-frequency Raman spectrum. It can be seen that the lattice modes exhibit a large pressure dependence as can be expected for molecular solids [22–25], except for the 68 and 77 cm^{-1} phonon peaks which are hardly pressure dependent with a pressure coefficient larger than 15 cm^{-1} GPa^{-1}. Figures 4(a) and (b) show plots of frequency versus pressure for five Raman-active lattice modes. The lowest-frequency mode is very weak and observed as a tail of the 37 cm^{-1} phonon peak. Consequently the determination of its pressure dependence suffers from low accuracy over a wide pressure range (3, 10 GPa) and thus the slope of its frequency shift was not reported in this range in table 1. Figures 4(a) and (b) reveal that all lattice modes exhibit a clear break in the slopes of the ω–P plots at about 2.5 GPa. In view of this, separate linear regressions were performed on the ω–P plots below and above 2.5 GPa. The results are reported in table 2. It can be seen that above 2.5 GPa, the frequency shifts are about 33–50% smaller than the initial slope in the ordered phase. Figure 3(a) reveals that the lattice modes are broadened above 5 GPa. The lineshape of the lattice modes appears asymmetric, as indicated by arrows in figure 3(a). Taking into account the drastic drop in intensity in this pressure range, we cannot be sure about the origin of this asymmetric lineshape. Two phenomena could be responsible for such a profile

of phonon peaks, which are fundamentally different. Local ordering in clusters could be responsible for asymmetric broadenings of the Raman lines [26, 27]. Alternatively, the splitting of Raman peaks into a non-resolved doublet could also explain this lineshape. Figures 3(b) and (c) reveal different Raman lineshapes of lattice modes at a given pressure for two different pressure runs. It is clearly observed that mode 5 appears very tailed at 7 GPa (figure 3(b)) for run 2, the lineshape being suggestive of split modes. With further compression (at 9 GPa; figure 3(c)), this mode becomes strangely less broadened and less tailed with increasing pressure. Comparative analysis of the Raman spectra taken in run 1 and run 2 indicates different lineshapes and thus different broadenings for a given lattice mode. This phenomenon is confirmed by the plot of the halfwidth at half-maximum (HWHM) discriminating between pressure runs (figure 5). In figure 5 a significant tendency towards broadening is clearly observed above 5 GPa. Above this pressure a clear non-reproducibility of these data is observed for two different runs in contrast to the case for the determination of frequencies using the same fitting procedure. Simultaneously with the broadening of the phonon peaks (above 5 GPa), one can observe that lattice modes gradually lose intensity with increasing pressure (figure 3(a)) and all lattice modes merge into the background above 6 GPa. When the pressure is released completely to atmospheric pressure, the reappearance of lattice modes of the disordered phase is observed.

(ii) The pressure dependence of the internal modes was analysed in the 200–250 cm^{-1} (figure 6(a)) and 390–500 cm^{-1} ranges (figure 6(b)). Figure 7 shows the pressure dependence of the internal-mode frequencies in the 200–500 cm^{-1} spectral range. All $(d\omega/dP)$ values are observed (table 2) also to be positive but drastically weaker than those determined for lattice modes. Below 3 GPa, internal modes exhibit linear pressure dependence, and thus the $(d\omega/dP)$ values reported in table 2 were determined from linear regression. All these values are observed to be drastically weaker than those of the lattice modes. Several $\omega(P)$ curves exhibit either a splitting into two bands or a break in the slope around 2.5–3 GPa. Above 6 GPa most of the internal modes display a similar drastic and positive $\omega(P)$ dependence. A detailed inspection of the high-pressure dependence of the Raman spectrum is presented in the bending-mode region (200, 250 cm^{-1}). The lowest-frequency internal band exhibits a very weak pressure dependence in contrast to the $\omega(P)$ behaviour of lattice modes and the high-frequency bending modes. This band broadens and splits into two components with increasing pressure. However, the two higher-frequency bands of the bending modes shift significantly with increasing pressure and merge into a broad band quasi-simultaneously with the splitting of the lower-frequency band. Over the whole pressure range, the pressure-induced frequency shift of the high-frequency bending mode is observed to be significantly larger than those of the other internal modes (table 2, figure 7(a)). This $\omega(P)$ dependence can be considered as an intermediate behaviour between those of external and internal modes. It can be observed that the two components of the bending modes exhibit a similar $\omega(P)$ behaviour above 5 GPa. These phenomena can be analysed on the basis of consideration of the temperature dependence of the two CN bending modes in the low-temperature phase of CNa [21]. Raman investigations in CNa have revealed a temperature independence of the low-frequency component (B_g mode corresponding to in-phase and out-of-plane bending) while the frequency of the other component (the A_g mode corresponding to an in-phase and in-plane bending) has a significant temperature dependence [21]. The temperature dependence of the frequency of the A_g mode was interpreted as resulting from the in-plane interaction between the CN of two neighbouring CNa molecules. Consequently the assignment of the Raman bands in the bending-mode region of Cla can be tentatively determined from the analysis of

their pressure dependence. The slight frequency shift with pressurization of the frequency of the low-frequency component in Cla suggests that this band corresponds to an out-of-plane C–C–Cl bending. Around 3 GPa, the additional component should correspond to an in-plane bending, like the higher-frequency component, taking into account their similar pressure-induced frequency shifts. The HWHM can be determinable for the lowest- and the highest-frequency bands, and is plotted versus P (figures 8(a) and (b)). A broadening is observed above 2 GPa both for the out-of-plane and in-plane bending modes while the lattice modes lose intensity. The quasi-independence of pressure of the bending modes in the low-pressure range ($P < 2$ GPa) suggests that the broadening would result from a frequency distribution rather than pressure-induced anharmonicity. It can be noted that the drastic broadening of the bending modes occurs simultaneously with the merging of the lattice modes in the background (above 9 GPa). The examination of the 400–500 cm^{-1} range also reveals the splitting of a Raman peak in the 2–3 GPa pressure range (figure 6(b)). As observed for the bending mode, the lowest-frequency component of the E mode exhibits a weak Raman shift with compression, whereas the other component has a pronounced pressure dependence characterized both by a large frequency shift and a splitting into two Raman peaks. The HWHM of the well-defined and non-split (A molecular) mode can be analysed (figure 8). Figure 8 shows that intramolecular modes exhibit roughly the same pressure dependence characterized by a severe increase above 9 GPa. Above 5 GPa, non-reproducible observations of the Raman lineshapes of phonon peaks for different pressure runs have been revealed.

4. Discussion

The comparison of both low- and high-frequency Raman spectra taken in the low-temperature and high-pressure phases suggests that the high-pressure ordered phase has the same crystal structure as the low-temperature phase, in agreement with a previous IR spectroscopic study [14] and as observed in adamantane [13]. Considering both the external-and internal-mode analyses, it is observed that the pressure-induced ordering process spreads over a relatively large pressure range (0, 0.55 GPa), whereas Cla undergoes a temperature-induced ordering process over a narrow temperature range. Raman features observed during the pressure-induced ordering process will be more easily understandable with the description of the temperature-induced ordering given on the basis of crystallographic data [19]. The orientational disorder of the molecules can be characterized by a tumbling motion of the C_3 molecular axis between the fourfold crystallographic axes in the $Fm3m$ space group, and a fast uniaxial rotation about the C_3 molecular axis. Below 210 K the tumbling motion is frozen, the molecule takes only one equilibrium position, and the C_3 molecular axis is fixed nearly in the planes $x = 1/4$ and $x = 3/4$ of the monoclinic unit cell ($P2_1/c$, $Z = 4$). In the orientationally ordered phase, the four molecules are locked in a distinct orientation. The C_3 molecular axes are orthogonal to each other and slightly tilted out the crystallographic planes. The temperature-induced phase transition was characterized by a significant decrease of the cell volume ($\Delta V/V = 6\%$) associated with the destructive nature of the phase transition.

It is worth pointing out that in both the high-pressure and low-temperature phases, a large number of expected Raman modes (from predictions given in table 1(a)) are not observed in the 400–500 cm^{-1} range. This discrepancy between the number of observed and predicted internal modes can be assigned to a roughly C_{1h} site symmetry. This hypothesis is supported by the observation of four components in the bending-mode region, since it is obvious that the C–C–Cl distortion is sensitive to the orientation of the C_3 axis.

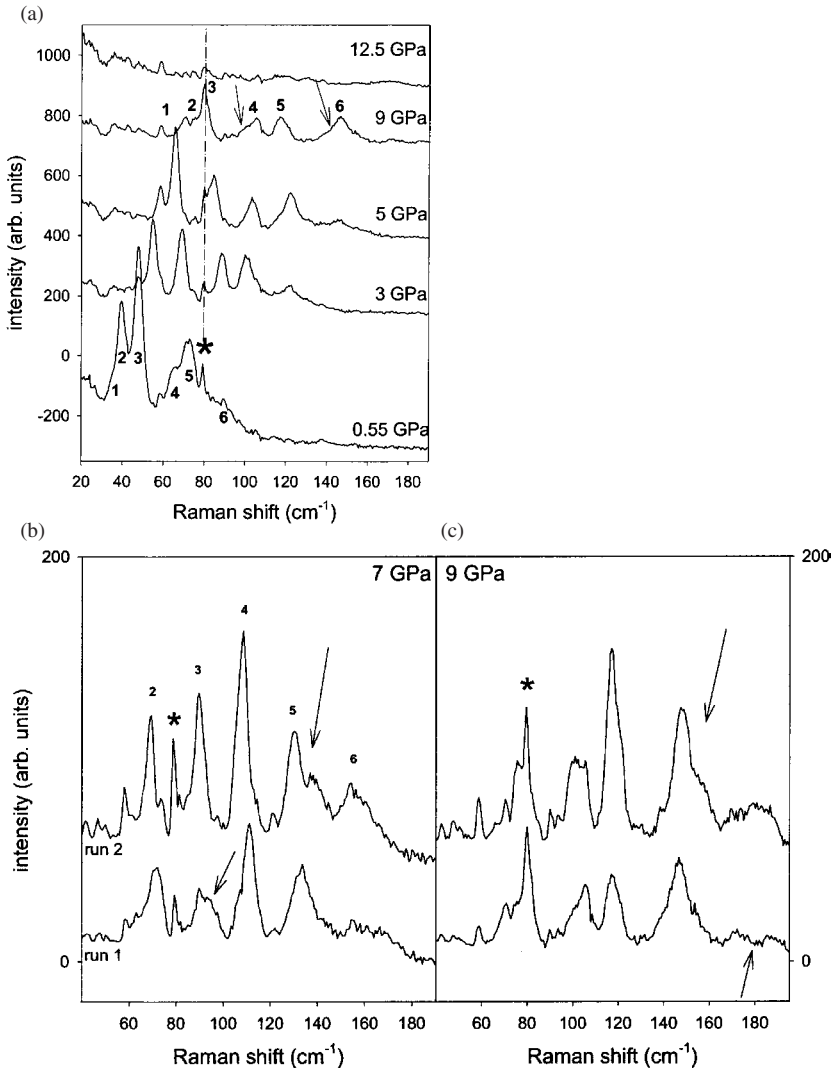

Figure 3. High-pressure dependence of the low-frequency Raman spectrum in the ordered phase of chloroadamantane. (a) The Raman spectra were taken in the same pressure run and the Raman lineshapes of the lattice modes are composed from spectra taken in two different pressure runs at 7 GPa (b) and at 9 GPa (c). The arrows indicate lattice modes which exhibit significantly different lineshapes for the two runs. The pronounced asymmetric lineshape of mode 5 (at 7 GPa; run 2) resembles two split modes. At 9 GPa (run 2) the Raman lineshape of this lattice mode appears strangely less asymmetric. The asterisk indicates the laser line.

The analysis of both $\omega(P)$ curves (figures 4 and 7) and $\mathrm{d}\omega/\mathrm{d}P$ values (table 2) reveals a drastic difference between the pressure dependence of external and internal modes. This strong discrepancy in the behaviour of intermolecular and intramolecular vibrations appears as a characteristic of molecular crystals [22–25]. In molecular crystals the intramolecular bonding is very strong compared to the weak intermolecular bonding. Consequently there is a disparity between force constants of molecular solids which is reflected in the Raman spectra, where internal modes are segregated from the low-frequency phonon peaks of the intermolecular

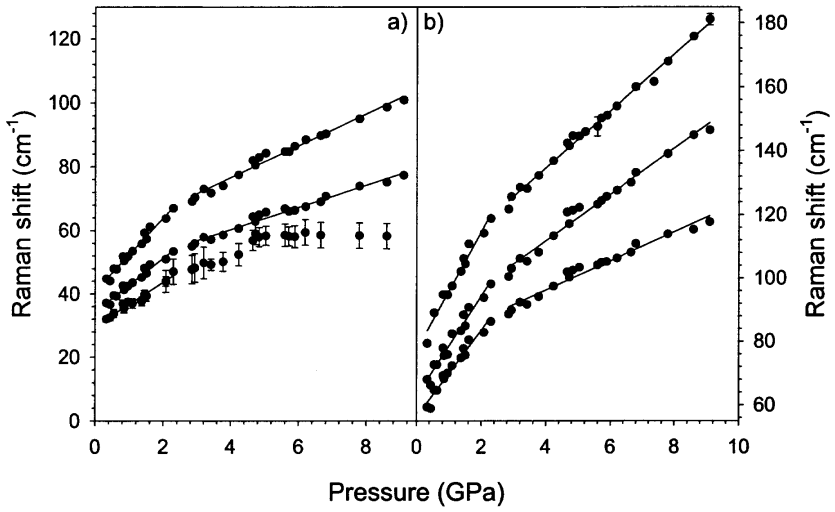

Figure 4. The pressure dependence of the lattice-mode frequencies in the ordered phase of Cla. Circles correspond to experimental data without discrimination between the three pressure runs, because of the satisfactory reproducibility of the data obtained by fitting Raman spectra. Lines correspond to linear regressions.

modes. Pressurization reduces the disparity between force constants, and thus also reduces the spectral gap between external and internal peaks. The intramolecular/intermolecular bonding anisotropy diminishes with compression and thus the molecular character does also. From these considerations, it can be easily understood that the frequencies of intermolecular modes increase rapidly with pressure, while the pressure dependence of the internal modes is much weaker. The high-frequency component of the internal bending mode exhibits a special $\omega(P)$ behaviour (characterized by $\mathrm{d}\omega/\mathrm{d}P \approx 6$ GPa cm^{-1}) clearly distinguishable from those of the external and internal modes (table 2).

A second characteristic of molecular crystals under pressure is the deviation from the vibrational scaling behaviour (called the Grüneisen approximation). The Grüneisen parameter γ_i connects the volume dilation $\Delta V/V$ with the fractional change in frequency by

$$\Delta\omega_i/\omega_i = -\gamma_i(\Delta V/V) = \gamma_i\beta P$$

where ω is the frequency, P the pressure, and β is the compressibility. Assuming all γ_i to be equal, Grüneisen approximation predicts a set of points, all lying on a horizontal line in a plot of $\log[(1/\omega_i)(\mathrm{d}\omega_i/\mathrm{d}P)]$ against $\log\omega_i$. This plot is reported for Cla in figure 9. These points fit correctly to the Grüneisen approximation in the external-mode region (in good agreement with results reported by Zallen and Slade for As_4S_4 [24]), i.e. the points are on a horizontal line while in the internal-mode region $\mathrm{d}(\ln\omega)/\mathrm{d}P$ decreases rapidly. This modification to the scaling law would be connected to the existence of disparate forces in a molecular crystal [24]. Moreover, Zallen and Slade [24] have predicted a bond-scaling exponent of -2 in the intramolecular regime controlled by an approximate inverse-square correlation between γ_i and ω_i. The fitting procedure in the intramolecular regime gives a slope of $-2.6(2)$ for Cla. This result demonstrates that the correlation $\gamma_i \propto \omega_i^{-2}$ can be considered as universal for molecular solids.

It can also be understood that the pressure-induced frequency shifts decrease with increasing pressure. This phenomenon is clearly observed for external modes through breaks in the slope of $\mathrm{d}\omega/\mathrm{d}P$. Table 2 reveals that the $\mathrm{d}\omega/\mathrm{d}P$ values of external modes considerably

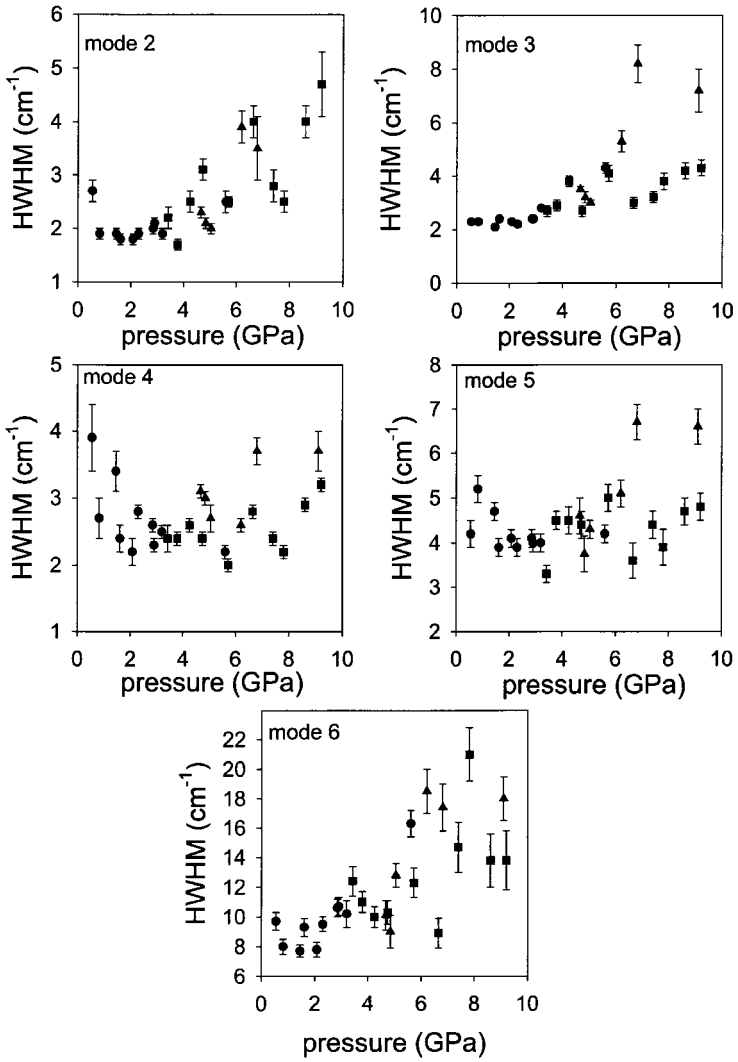

Figure 5. The pressure dependence of the Raman linewidths of lattice modes in the ordered phase of chloroadamantane. Circles correspond to run 1, triangles to run 2, and squares to run 3. No data are reported for mode 1 because of its low Raman definition.

decrease above 2.5–3 GPa. In the same pressure range, the $\omega(P)$ curves flatten out in the internal-mode region. Above this pressure it can be considered that the behaviour of Cla under pressure becomes close to that of covalent-network crystals, i.e. the spectral gap between external and internal modes is reduced. This spectral gap is analysed in figure 10 and also through the quantity $[(\omega_{int}^{min}/\omega_{ext}^{max}) - 1]$ introduced by Zallen and Slade [24], where ω_{int}^{min} corresponds to the lowest internal-mode frequency and ω_{ext}^{max} to the highest external-mode frequency. This quantity is halved from 1.1 to 0.2 upon passing from $P = 0.5$ to $P = 9$ GPa. Figure 10 shows that the spectral gap appears as indefinitely reducible until overlapping occurs between external and internal modes at 10 GPa. At this high pressure, mode 6 is very flattened and quasi-unobservable; however, the large pressure-induced frequency shift of this mode suggests that it could overlap with bending modes. Such a narrowing of the gap between

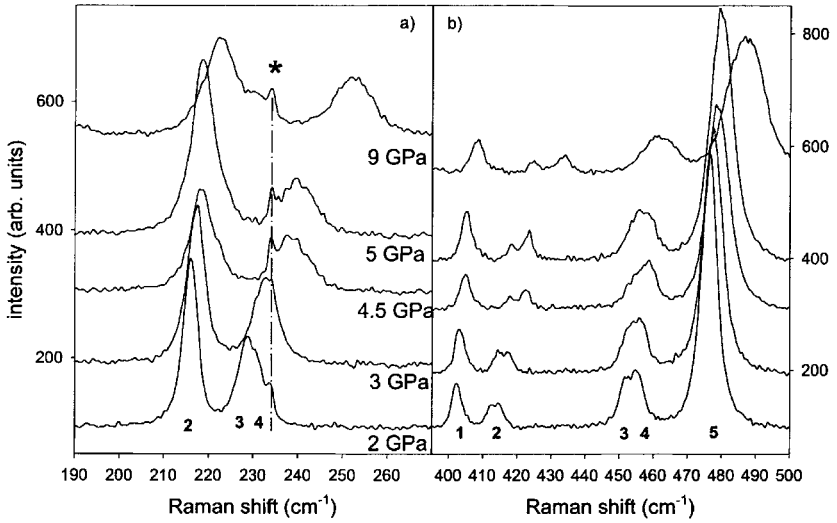

Figure 6. Raman spectra in the ordered phase of Cla taken at various pressures in run 1: (a) in the bending-mode region (the asterisk indicates the laser line); (b) in the 390–500 cm^{-1} range.

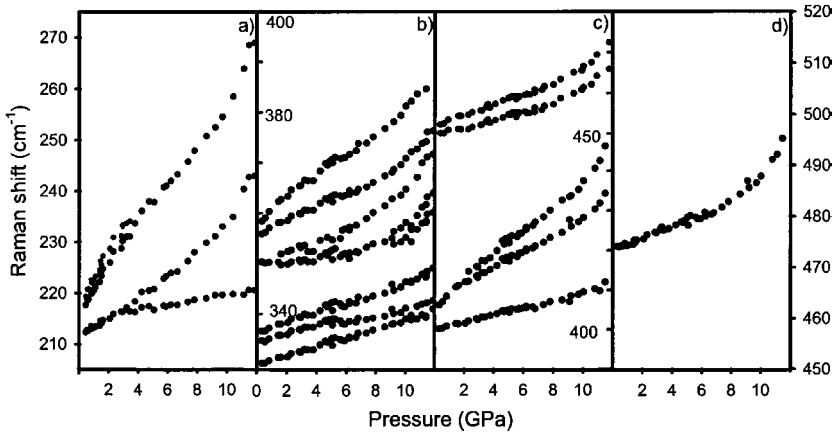

Figure 7. The pressure dependence of internal-mode frequencies in the 210–500 cm^{-1} range of the ordered phase of Cla.

external and internal modes could be a special spectroscopic feature of plastic crystals enhanced in Cla. It is worth pointing out that Cla is well known for its high ductility, obviously associated with the feature of being easily compressible.

Above 2.5–3 GPa, splittings of internal modes are also observed in several spectral regions. It is well known that pressure enhances the spectroscopic consequences of the intermolecular interactions such as the Davydov splittings of the intramolecular-mode frequencies, and thus the observation of additional internal modes can be understood as the enhancement of Davydov splittings corresponding to non-resolved doublets because of the rough C_{1h} site symmetry. Alternatively, the reduction of volume inherent to pressurization could be responsible for local orientational ordering, and thus for changes in the nearest neighbours of a Cla molecule. Such a phenomenon could be the origin of more extra-activated modes at pressure above 3 GPa.

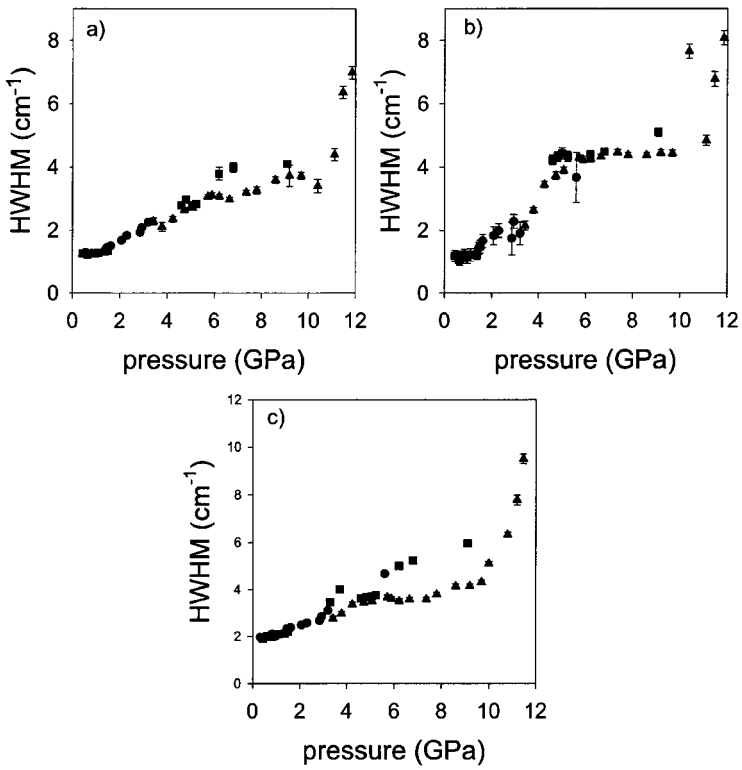

Figure 8. Pressure dependences of the linewidths of some internal modes: (a) the low-frequency component of the (E molecular) bending mode; (b) the high-frequency component of the bending mode; (c) the most intense band in the 390–500 cm^{-1} region (A_1 molecular symmetry).

From the structural description of the low-temperature phase [19], the origin of the splittings can reasonably be assigned as the enhancement of the tilting of the C_3 molecular axes out of the crystallographic planes, since this tilting is responsible for the loss of the mirror plane in the site symmetry, i.e. the C_1 group. Splittings of internal modes have also been observed by IR spectroscopy [14] around 1.7 GPa and have been interpreted as the signature of a phase transition in a more ordered phase. However, no additional lattice mode was detected in this pressure range. Consequently, the interpretation of splittings of internal modes in terms of new high-pressure phase appears not to be convincing, despite the observation of changes in the pressure dependence of intermolecular- and intramolecular-mode frequencies in the same pressure range. Raman features around 2.5–3 GPa can also be described as the manifestation of the pressure effect upon intermolecular force constants.

At higher pressure ($P > 6$ GPa) lattice modes exhibit an asymmetric and non-reproducible lineshape and drop in intensity (figure 3(a)). In the same pressure range the frequency for most of the intramolecular modes exhibits an unusual non-linear and positive pressure dependence in this high-pressure range. The analysis of the bending-mode region reveals also a broadening of the low- and high-frequency components above 2 GPa and a more drastic one above 9 GPa (figure 8). The first increase of the linewidths of some internal modes (figure 8) in the pressure range where splittings of internal modes are observed is suggestive of an inhomogeneous ordering, since such splittings are associated with disorder–order phase transition. This broadening of internal modes while the lattice modes lose intensity and

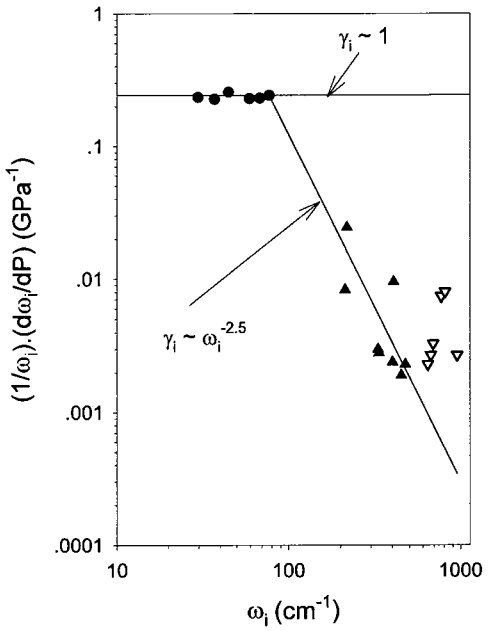

Figure 9. A log–log presentation of the phonon-mode frequency shift with pressure against mode frequency representative of the vibrational scaling behaviour in molecular crystals. The two different behaviours determined for the Grüneisen parameter corresponding to external and internal modes reflect the disparity in bonding forces [23]. Full circles correspond to lattice modes and triangles to internal modes. Full upward-pointing triangles are obtained from the present study, whereas open downward-pointing triangles are taken from [14].

merge into the background can be associated with similar observations for resorcinol which have been interpreted as an amorphization [28]. In a recent study [25], these phenomena were interpreted as a phase transition into a disordered phase. In the present study, the drop in intensity accompanied with an asymmetric broadening of lattice modes (figure 3) and internal modes (figure 6) could also be tentatively interpreted as the progressive loss of the long-range order (LRO) because of the tendency of the system to achieve closer packing. The non-reproducible Raman lineshapes in different pressure runs can be considered as experimental evidence for metastable states above 5–6 GPa. The Raman lineshape of the bending modes observed at 9 GPa, i.e. the asymmetric broadening associated with the emergence of an additional broad component, can be considered as the signature of micro-domains of an ordered structure denser than the original one. This phenomenon would cause the formation of a metastable state composed of ordered domains characterized by local structure denser than the original LRO, where the C_3 molecular axes would be significantly tilted out the $x = 1/4$ and $x = 3/4$ crystallographic planes. The disappearance of lattice modes with further pressure increase would then correspond to a severe decrease of the size of the clusters of the ordered phases, i.e. a pressure-induced amorphization. These phenomena were observed to be reversible, indicating that intramolecular and intermolecular bondings are not altered drastically. On the other hand, the temperature-induced order–disorder transition is destructive [19], and thus the sample is expected to break into microcrystalline domains near 0.6 GPa. Consequently, further compression can generate a high density of dislocations and considerable stress inhomogeneity on the scale of the domain size ($\approx$1 μm) which cannot be detected from the three ruby chips included in the cell. Such a situation is also consistent

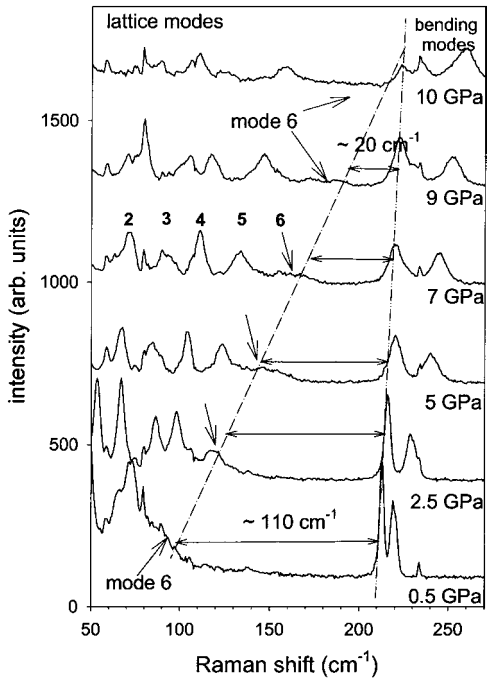

Figure 10. A representation of the narrowing of the spectral gap between external and internal modes against pressure. The dashed lines can be used as a guide for the eyes, giving a rough representation of the pressure-induced frequency shifts for the two kinds of vibration modes.

with the special Raman features observed with high pressurization, i.e. the increase of Raman linewidths of internal modes which could be inherent to a pressure gradient within the sample, and the disappearance of external modes which could result from a strong elastic scattering.

5. Conclusions

We have shown that Cla plastic crystal exhibits characteristic spectroscopic features observed in molecular crystals under pressure. The most striking feature lies in the strong discrepancy between pressure-induced frequency shifts of external and internal modes. This feature appears enhanced in Cla with respect to other molecular crystals [22–25]. However, figure 9 demonstrates that frequency shifts of lattice modes follow the Grüneisen approximation and the behaviour of internal-mode frequencies is roughly in agreement with a quasi-universal scaling law for molecular solids [24]. Figure 10 appears well adapted to summarize the main spectroscopic features of the Cla plastic crystal under pressure. The contrast between the pressure behaviours of external and internal modes is clearly observed. The frequency shift of the internal modes appears as insignificant in comparison to the large pressure-induced frequency shift of the lattice modes, whereas internal modes exhibit considerable broadening (compared with the lattice modes).

The present study reveals that the pressurization of the disordered phase generates an ordering process which spreads over a relative wide pressure range. The ordering process can be reasonably interpreted in terms of achievement of closer packing, i.e. as a reduction of volume. The first observed stage is the disorder–order phase transition. Then, with further pressurization

the system continues to achieve closer packing. From the observation of splittings of about 3 GPa interpreted as inherent to the tilting of the C_3 molecular axes out the crystallographic planes, a close-packed local ordering can be described as the pronounced tilting of molecules reducing the volume of the molecular surroundings. The broadening of the internal modes above 2 GPa (figure 8) suggests an inhomogeneous ordering. In this context the disappearance of the external modes around 12 GPa can be tentatively explained as follows. Since there is no LRO denser than the known monoclinic structure, micro-ordered domains where the local structure is denser than the LRO are formed. A metastable state thus results from the breaking of the LRO. An ambiguous situation is then obtained during the ordering process by pressurization, in which the system evolves into a disordered metastable state composed from 'ultra'-ordered domains forming a compact configuration which possesses no LRO. The tendency towards broadening of external modes above 5 GPa (figure 5) can be interpreted as the signature of the progressive loss of the LRO.

Despite such a statement having already been made regarding a molecular material [27] with similar Raman features, the consideration of strong elastic scattering of the incident light resulting from a high dislocation content is also a scenario consistent with the Raman features observed above 8 GPa. To give a more precise description of the pressure-induced ordering process in the high-pressure range, Raman investigations under pressure on other substituted adamantane compounds are needed and will be performed very soon.

References

[1] Descamps M and Caucheteux C 1987 *J. Phys. C: Solid State Phys.* **20** 5073
[2] Criado A *et al* 2000 *Phys. Rev.* B **61** 12 082
[3] Benkhof S, Kudlik A, Blochowicz T and Rössler E 1998 *J. Phys.: Condens. Matter* **10** 8155
[4] Brand R, Lunkenheimer P and Loidl A 1997 *Phys. Rev.* B **56** R5713
[5] Krüger J K *et al* 1994 *J. Phys.: Condens. Matter* **6** 6947
[6] Angell C A *et al* 1985 *J. Chim. Phys.* **82** 767
[7] Angell C A 1991 *J. Non-Cryst. Solids* **131–133** 13
[8] Affouard F and Descamps M 2001 *Phys. Rev. Lett.* **87** 035501
[9] Affouard F, Cochin E, Decressain R and Descamps M 2001 *Europhys. Lett.* **53** 611
[10] Affouard F, Hédoux A, Guinet Y, Denicourt T and Descamps M 2001 *J. Phys.: Condens. Matter* **13** 7237
[11] Sastry S, Denedetti P G and Stillinger F 1998 *Nature* **393** 54
[12] Nordman C E and Schmitkons D L 1965 *Acta Crystallogr.* **18** 764
[13] Rao R *et al* 2000 *J. Chem. Phys.* **112** 6739
[14] Fraczyk L A and Huang Y 2001 *Spectrochim. Acta* A **57** 1061
[15] Snoke D W, Raptis Y S and Syassen K 1992 *Phys. Rev.* B **45** 14 419
[16] Chandrabhas N *et al* 1994 *Phys. Rev. Lett.* **73** 3411
[17] Mishima O and Stanley H E 1998 *Nature* **396** 329
[18] Katayama Y *et al* 1998 *Nature* **403** 170
[19] Piermarini G J and Block S 1975 *Rev. Sci. Instrum.* **46** 973
[20] Foulon M, Belgrand T, Gors C and More M 1989 *Acta Crystallogr.* B **45** 404
[21] Guinet Y and Sauvajol J L 1988 *J. Phys. C: Solid State Phys.* **21** 3827
[22] Besson J M, Thiery M M and Pruzan Ph 1991 *Molecular System Under Pressure* ed R Pucci and G Piccito (Amsterdam: Elsevier) p 341
[23] Zallen R 1974 *Phys. Rev.* B **9** 4485
[24] Zallen R and Slade M L 1978 *Phys. Rev.* B **18** 5775
[25] Rao R, Sakuntala T and Godwal B K 2002 *Phys. Rev.* B **65** 54 108
[26] Pevtsov A B *et al* 1995 *Phys. Rev.* B **52** 955
[27] Toulouse J, DiAntonio P, Vugmeister B E, Wang X M and Knauss L A 1992 *Phys. Rev. Lett.* **68** 232
[28] Deb S K, Rekha and Roy A P 1993 *Phys. Rev.* B **47** 11 491